Secure data collection via UAV-carried IRS

Journal Pre-proof

Secure data collection via UAV-carried IRS

Christantus O. Nnamani, Muhammad R.A. Khandaker,
Mathini Sellathurai

PII: S2405-9595(22)00136-9
DOI: https://doi.org/10.1016/j.icte.2022.09.003
Reference: ICTE 548

To appear in: *ICT Express*

Received date : 16 March 2022
Revised date : 17 August 2022
Accepted date : 2 September 2022

Please cite this article as: C.O. Nnamani, M.R.A. Khandaker and M. Sellathurai, Secure data collection via UAV-carried IRS, *ICT Express* (2022), doi: https://doi.org/10.1016/j.icte.2022.09.003.

Title Page (with Author Details)

Secure Data Collection via UAV-Carried IRS

Christantus O. Nnamani*, Muhammad R. A. Khandaker, Mathini Sellathurai

Christantus Nnamani, Muhammad Khandaker and Mathini Sellathurai are with the School of Engineering and Physical Sciences, Heriot-Watt University, Edinburgh EH14 4AS, United Kingdom.

*Correspondence to: School of Engineering and Physical Sciences, Heriot-Watt University, Edinburgh EH14 4AS, United Kingdom. E-mail address: con1@hw.ac.uk or obinna.nnamani@unn.edu.ng

This work was supported in part by the EPSRC Project EP/P009670/1, Petroleum Technology Development Fund (Grant number: PTDF/ED/PHD/NCO/1352/18) and University of Nigeria Nsukka.

Secure Data Collection via UAV-Carried IRS

Christantus O. Nnamani[1*], Muhammad R. A. Khandaker[2], Mathini Sellathurai[3]
[1,2,3]School of Engineering and Physical Sciences, Heriot-Watt University, Edinburgh EH14 4AS, UK.
*Correspondence to con1@hw.ac.uk, obinna.nnamani@unn.edu.ng

This work was supported in part by the EPSRC Project EP/P009670/1, Petroleum Technology Development Fund (Grant number: PTDF/ED/PHD/NCO/1352/18).

***Abstract*— This paper considers unmanned aerial vehicle (UAV)-carried intelligent reflecting surface (IRS) for secure data collection in wireless sensor networks. An eavesdropper (Eve) lurks within the vicinity of the main receiver (Bob). Several distributed sensors beamform collaboratively to the UAV-carried IRS reflecting the signal to the main receiver (Bob). The design objective is to maximize the achievable secrecy rate in noisy communication channel by optimizing the collaborative beamforming weights of the sensors, trajectory of the UAV and reflection coefficients of the IRS elements. We proposed novel method to obtain the parameters using non-iterative approach by mitigating the IRS reflection coefficients dependencies.**

***Index Terms*—Secure communication, IRS, UAV, optimization, physical layer security.**

I. Introduction

With the proliferation of computing capabilities as well as wireless internet of things (IoT) applications in 5G, security of communications is becoming increasingly vulnerable to external threats [1], [2]. Accordingly, additional security measures including lightweight cryptography [1] and physical layer security (PLS) [2] have been proposed, particularly for resource-constrained IoT devices. PLS was further improved by using multiple collaborative intermediary relay nodes [3], [4]. Although the relay nodes therein were active, the structure alludes to the use of passive intelligent reflecting surfaces (IRS) system. Recently, IRS enabled programmable wireless channels was proposed to dispense PLS as practical solution to communication security [5], [6]. However, the reflected signal from the IRS cannot be said to be specular within the radio spectrum due to the dependence of its beamwidth on the wavelength and IRS plate width [7]. This implies that some weak reflected signal will leak to the surrounding of the intended receiver, thereby allowing for possible eavesdropping. This worsen if the eavesdropper statistics are unknown. Although, due to the manipulation of the wireless channel to be favorable at desired location and adverse at another, the PLS of the IRS-aided communication is substantially better than modern conventional communication [5], [8]. However, by optimizing the reflection coefficients, PLS can substantially improve [8].

One key feature of the secrecy IRS system is that the reflected signals can be made to constructively combined at the legitimate receiver, while acting destructively at the eavesdropper. But if the IRS placement is not be optimal especially due to its fixed nature [9], the performance in terms of PLS will be reduced. Most of the existing works on IRS-aided communication focus on fixed terrestrial IRS deployment (on facades of buildings or indoor walls/ceilings). This fixed deployment does not provide adaptability to mobile users and does not reap the full potential of IRS in terms of information rate and PLS. It is desirable to allow mobility of the IRS system possibly by mounting it on a UAV or other aerial devices [9], [10]. The choice of aerial mobility system also allows for the exploitation of aerial visibility for the IRS line-of-sight (LoS) application. One major drawback of aerial IRS is that more malicious users can also establish LoS link between the aerial IRS system, and relying on the non-specular nature of the reflected radio signal, compromise the secrecy of the communication. The PLS of a collaborative transmitting sources reflected via an aerial IRS has not been examined in the literature to the best of our knowledge. However, an uplink time-based users scheduling for communication via aerial IRS was presented in [10]. This differs from our work since we are employing distributed beamforming and exploring a simplified non-iterative approach.

The objective of this paper is to secure data transmission with a UAV-carried IRS system in a noisy multi-sensory scenario. We note that the sensory data maybe obtained from pipeline monitoring, or any other sensory application functioning via multiple nodes. By maximizing the achievable average secrecy rate under total transmit power constraint, we optimize the transmit beamforming weights, IRS reflection coefficients and the location of the IRS system aided by the mobility of the UAV. We assume that there were no direct link between the sensors and the base station (BS), therefore the communication link was established only through the UAV-carried IRS system. The major contributions of this paper are:

a) We design the IRS reflection coefficients, beamforming weights and UAV trajectory considering when the eavesdropper is active and passive.
b) Considering a noisy environment, we proposed an analytical derivation of the signal-to-noise ratio (SNR) at the main receiver and at the eavesdropper.

To the best of our knowledge, no other existing work has investigated aerial/mobile IRS for secure communications with the direction presented herein.

II. System Model and Problem Formulation

Consider an IRS system with K elements carried on a UAV tracing a path, such that the reflected signals from M ground sensors (Alice) distributed over r radius were received at an LoS incommunicado base station (Bob). However, an eavesdropper (Eve) listens to the reflected transmission. Let the 3D location of Bob, Eve, and the center of Alice were denoted as $\mathbf{\Omega}_{\mathrm{B}}$, $\mathbf{\Omega}_{\mathrm{E}}$, $\mathbf{\Omega}_{\mathrm{A}}$, respectively. The entire flight time (T) of the UAV be sampled at discrete time-stamps of N equal time slots, with duration $\alpha = \frac{T}{N}$. We note that as

$N \to \infty$, the UAV is seen to follow a continuous trajectory $\mathbf{Q} = [\mathbf{q}[1], \ldots, \mathbf{q}[N]]$, thereby satisfying time-sharing conditions and transmitting continuously over T [11], [12]. The channels within 2 successive slots relating to the UAV-IRS system are assumed to vary slowly allowing for block fading.

Without loss of generality, we assume that the UAV flies at a constant altitude H and a maximum speed of Zm/s within α seconds. Therefore its nth location is $\mathbf{q}[n] = [q_{\mathrm{x}}[n], q_{\mathrm{y}}[n], H]^{\mathrm{T}}, \forall\ n \in \{1, \ldots, N\}$. The kth IRS element is located at $\mathbf{q}_k[n] = [q_{\mathrm{Rx}}[n] + (k_{\mathrm{x}} - 1)d_{\mathrm{x}}, q_{\mathrm{Ry}}[n] + (k_{\mathrm{y}} - 1)d_{\mathrm{y}}, H]^{\mathrm{T}}, \quad \forall\ k_{\mathrm{x}} \in \{1, \ldots, K_{\mathrm{x}}\},\ k_{\mathrm{y}} \in \{1, \ldots, K_{\mathrm{y}}\}$, where K_{x}, K_{y}, d_{x} and d_{y} define the number of IRS elements and the spaces in-between along the x- and y-directions of the grid respectively. $\{d_{\mathrm{x}},\ d_{\mathrm{y}}\} \leq \lambda$ to avoid a far field mismatch between the desired reflection angle and the IRS array response [7]. Without loss of generality, we set a reference location of a particular IRS element to be the same as the trajectory of the UAV such that $\mathbf{q}_{\mathrm{R}}[n] = \mathbf{q}[n]$.

If Alice collaboratively transmits unique symbols $s(t)$ with $\mathbb{E}\{|s(t)|^2\} = 1$ over T_s snapshots, then $x(t) = s(t)\exp(j\omega_c t)$ becomes the modulated signal for $t \in \{1, \ldots, T_s\}$. Let $\mathbf{g}_m = [g_{m1}, g_{m2}, \ldots, g_{mK}]^{\mathrm{T}}$ denote the IRS to the mth sensor complex channel vector, and w_m represents the beamforming weight of the mth sensor of Alice (for $m \in \{1, \ldots, M\}$). Thus, the complex channel matrix between the IRS elements and all the sensors on Alice is $\mathbf{G} = [\mathbf{g}_1, \mathbf{g}_2, \ldots, \mathbf{g}_M] \sim \mathcal{C}^{K \times M}$. Invariably, the mth incident signal on the kth element is (1).

$$g_{mk}[n]w_m[n]\mathrm{x}(t) = \mathrm{Re}\{w_m\sqrt{c_{m\mathrm{R}}[n]}\exp\left(-j\phi_{mk}[n]\hat{\mathbf{a}}_{m\mathrm{R}}\right) \times \delta\left(t - \frac{\phi_{mk}[n]}{\omega_{\mathrm{c}}}\right)s(t)\exp\left(j\omega_{\mathrm{c}}t\right)\}, \quad (1)$$

where ω_{c} is the angular frequency and $\phi_{mk} \coloneqq \omega_{\mathrm{c}}\tau_{mk}$ defines the coordinate spatial frequency and the phase shift between the kth IRS element and the mth sensor. $c_{mk}[n]$ is the channel gain. In the rest of the paper, we define the channel gains as $c_{ij}[n] \coloneqq \frac{\rho_0 \varsigma}{\|\mathbf{q}_j[n] - \Omega_i\|^2}$ for ρ_0 representing channel power at reference distance $d_0 = 1$m and ς denoting an exponentially distributed random variable with unit mean. $\hat{\mathbf{a}}_{ij} \coloneqq \frac{\mathbf{a}_j - \mathbf{a}_i}{\|\mathbf{a}_j - \mathbf{a}_i\|}$ is a normalized vector along the propagation path.

Although the inter-spacing of the IRS elements and that of the sensors are less than the distance between the UAV and Alice, the unique sensors to IRS elements variation cannot be ignored. This is primarily due to the possible large inter-space between some sensors especially in multi-faceted environment. However, the beam from the sensors is collaboratively directed to the UAV-IRS system using distributed array formation and controlled with the phase shift given in (2).

$$\phi_{mk}\hat{\mathbf{a}}_{m\mathrm{R}} \approx \underbrace{\frac{2\pi}{\lambda}\|\mathbf{q}_{\mathrm{R}} - \mathbf{\Omega}_m\|}_{\phi^a_{m\mathrm{R}}} + \underbrace{\frac{2\pi\hat{\mathbf{a}}_{m\mathrm{R}}}{\lambda}\|\mathbf{q}_k - \mathbf{q}_{\mathrm{R}}\|\hat{\mathbf{a}}_{Rk}}_{\phi^b_{mk}}. \quad (2)$$

It is imperative, then, that from (2), the phase shift was comprised of two distinct parts; based on i) fixed phase ($\phi^a_{m\mathrm{R}}$) and ii) variable phase (ϕ^b_{mk}). While the fixed phase relates the IRS on the UAV to the transmitter, the variable phase describes the correlation between the IRS elements. In component form, the kth IRS element response phase can be written as (3)

$$\phi^b_{mk} = [(k_{\mathrm{x}} - 1)\bar{d}_{\mathrm{x}}, (k_{\mathrm{y}} - 1)\bar{d}_{\mathrm{y}}, 0] \cdot [\hat{\mathbf{a}}^x_{m\mathrm{R}}, \hat{\mathbf{a}}^y_{m\mathrm{R}}, \hat{\mathbf{a}}^z_{m\mathrm{R}}]^{\mathrm{T}}, \quad (3)$$

where $\bar{d}_{\mathrm{x}} = \frac{2\pi d_{\mathrm{x}}}{\lambda}$ and $\bar{d}_{\mathrm{y}} = \frac{2\pi d_{\mathrm{y}}}{\lambda}$. It is easy to deduce that the IRS array response to all the sensor nodes can be represented with a $K \times M$ matrix, $\mathbf{\Phi}_{\mathrm{G}}$, whose elements are given in (3).

By extracting the nth complex channel coefficients from (1), the complex channel between the kth IRS element and the mth sensor node in Alice was thus presented as

$$g_{mk} = \sqrt{c_{m\mathrm{R}}}\exp\left(-j\phi^a_{m\mathrm{R}}\right)\exp\left(-j\phi^b_{mk}\right)\delta\left(t - \frac{\phi_{mk}}{\omega_{\mathrm{c}}}\right), \quad (4)$$

Similarly, the nth complex channel between the IRS and the ground nodes ($\mathbf{h}_{\mathrm{i}} = [h_{1i}, \ldots, h_{K\mathrm{i}}]^{\mathrm{T}} \sim \mathcal{C}^{K\times 1}, \forall\ \mathrm{i} \in \{\mathrm{B}, \mathrm{E}\}$ where B and E represents Bob and Eve respectively), was obtained in (5) by updating the direction of the reflected signal.

$$h_{k\mathrm{i}} = \sqrt{c_{\mathrm{Ri}}}\exp\left(-j\phi^a_{\mathrm{Ri}}\right)\exp\left(-j\phi^b_{k\mathrm{i}}\right)\delta\left(t - \frac{\phi_{k\mathrm{i}}}{\omega_{\mathrm{c}}}\right), \quad (5)$$

where $\phi^b_{k\mathrm{i}} = [(k_{\mathrm{x}} - 1)\bar{d}_{\mathrm{x}}, (k_{\mathrm{y}} - 1)\bar{d}_{\mathrm{y}}, 0] \cdot [\hat{\mathbf{a}}^x_{\mathrm{Ri}}, \hat{\mathbf{a}}^y_{\mathrm{Ri}}, \hat{\mathbf{a}}^z_{\mathrm{Ri}}]^{\mathrm{T}}$ and $\phi^a_{\mathrm{Ri}} = \frac{2\pi}{\lambda}\|\mathbf{\Omega}_{\mathrm{i}} - \mathbf{q}_{\mathrm{R}}\|$.

Therefore, the coherently received signal at the ground nodes (Bob and Eve) during the nth sample was given by

$$y_{\mathrm{i}} = \mathbf{h}_{\mathrm{i}}^{\mathrm{H}}\mathbf{\Theta}\mathbf{G}\mathbf{w}\mathrm{x}(t) + \eta_{\mathrm{i}}, \quad (6)$$

where $\mathrm{i} \in \{\mathrm{B}, \mathrm{E}\}$, $\mathbf{w} = [w_1, \ldots, w_M]^{\mathrm{T}}$ is the beamforming weights, $\mathbf{\Theta} = \mathrm{diag}(\exp(j\theta_1), \exp(j\theta_2), \ldots, \exp(j\theta_K))$ represents the vectorized reflection coefficients of the IRS elements and $\eta_{\mathrm{i}} \sim \mathcal{CN}(0, \sigma^2_{\mathrm{i}})$ presents an independent and identically distributed (i.i.d.) additive white Gaussian noise (AWGN) at the corresponding receiver. Recall that at the ground receiver nodes, (Bob and Eve), the reflected signals from all the IRS elements are superimposed coherently [8], [9]. It is intended that such coherent superimposition will maximize the received signal power at the Bob while limiting the signal power at Eve.

We therefore formulate our problems under these subheadings.

1) Generic approach:: Given the channel information of Bob and Eve, we aim to maximize the secrecy rate of the communication. Accordingly, we formulate the following optimization problem:

$$\mathrm{P1a}: \max_{\mathbf{w},\mathbf{Q},\mathbf{\Theta}} \frac{1}{N}\sum_{n=1}^{N}\left[\log_2\left(\frac{1 + \gamma_{\mathrm{B}}[n]}{1 + \gamma_{\mathrm{E}}[n]}\right)\right]^+, \quad (7a)$$

$$\text{s.t. } 0 \leq \theta_k[n] \leq 2\pi, \quad (7b)$$

$$\|\mathbf{q}[n] - \mathbf{q}[n-1]\|^2 \leq (Z\alpha)^2 \quad (7c)$$

$$\mathbf{w}[n]^{\mathrm{H}}\mathbf{w}[n] \leq P, \quad (7d)$$

where $\gamma_{\mathrm{i}}[n] = \frac{1}{\sigma^2_{\mathrm{i}}}|\mathbf{h}_{\mathrm{i}}^{\mathrm{H}}[n]\mathbf{\Theta}[n]\mathbf{G}[n]\mathbf{w}[n]|^2,\ \mathrm{i} \in \{\mathrm{B}, \mathrm{E}\}$ represents the signal to noise ratio at Bob and Eve. $[x]^+ = \max\{\mathrm{x}, 0\}$ Note that negative objective will not arise in this model because there are no direct paths between Alice and Bob/Eve. The constraint in (7b) ensures that the principal argument of the reflection coefficient from the kth IRS was maintained while (7c) and (7d) limits the distance covered by the UAV between sampling points and total sensor power respectively.

2) Modified approach:: Given that the presences of Eve in the system model is unknown, we aim to maximize the rate achieved at Bob by solving problem P1b and evaluate the impact of passive Eve.

$$\text{P1b}: \max_{\mathbf{w},\mathbf{Q},\boldsymbol{\Theta}} \frac{1}{N}\sum_{n=1}^{N}[\log_2(1+\gamma_{\mathrm{B}}[n])]^{+}, \tag{8a}$$

$$\text{s.t. } 0 \le \theta_k[n] \le 2\pi, \tag{8b}$$

$$\|\mathbf{q}[n]-\mathbf{q}[n-1]\|^2 \le (Z\alpha)^2 \tag{8c}$$

$$\mathbf{w}[n]^{\mathrm{H}}\mathbf{w}[n] \le P, \tag{8d}$$

Considering that when the eavesdropper is passive, no information or estimates about its location or channel distribution is available. Hence, γ_{E} cannot be modeled correctly. The focus therefore becomes to maximize the achievable rate at Bob.

III. Proposed Solution

In this section, we present the solution to problems P1a and P1b by solving simplified sub-problems for each optimization parameter. We note that since block fading exist between the successive n slots, the channel do not change significantly within successive slots to alter the designs of the beamforming and reflection coefficients as discussed herein.

A. Solving for the reflection coefficients, $\boldsymbol{\Theta}$

We present the solutions to problems P1a and P1b given that the beamforming vectors, $\mathbf{w}$, and the trajectory of the UAV, $\mathbf{Q}$, are known.

1) Generic approach: The sub-problem from problem P1a in relation to $\boldsymbol{\Theta}$ reduces to problem P2a

$$\text{P2a}: \max_{\boldsymbol{\Theta}} \frac{1}{N}\sum_{n=1}^{N}\left[\log_2\left(\frac{1+\gamma_{\mathrm{B}}[n]}{1+\gamma_{\mathrm{E}}[n]}\right)\right], \tag{9a}$$

$$\text{s.t. } 0 \le \theta_k[n] \le 2\pi. \tag{9b}$$

Problem P2a is non-convex but by applying some matrix manipulations, such that $\gamma_i = |\frac{1}{\sigma_i^2}\mathbf{h}_{\mathrm{i}}^{\mathrm{H}}\boldsymbol{\Theta}\mathbf{G}\mathbf{w}|^2 = |\frac{1}{\sigma_i^2}\hat{\boldsymbol{\theta}}^{\mathrm{H}}\mathbf{H}_{\mathrm{i}}\mathbf{G}\mathbf{w}|^2 \;\; \forall\, i \in \{\mathrm{B},\mathrm{E}\}$, where $\hat{\boldsymbol{\theta}} = [\exp(j\theta_1),\ldots,\exp(j\theta_K)]^{\mathrm{H}}$ and $\mathbf{H}_i = \mathrm{diag}(\mathbf{h}_{\mathrm{i}}^{\mathrm{H}})$. The constraint in (9b) has been rewritten For tractability, (9b) becomes (10b) since the square magnitude of a complex exponent is 1. It is easy to see that the problem defined in problem P2a is not dependent on the nth sample, hence we can be solved for each n. Therefore a modified semi-definite programming (SDP) problem of P2a is given in (10).

$$\max_{\hat{\boldsymbol{\Theta}}} \left(\frac{1+\mathrm{Tr}(\mathbf{A}\hat{\boldsymbol{\Theta}})}{1+\mathrm{Tr}(\mathbf{B}\hat{\boldsymbol{\Theta}})}\right), \tag{10a}$$

$$\text{s.t. } \mathrm{diag}(\hat{\boldsymbol{\Theta}}) = 1, \tag{10b}$$

$$\mathrm{rank}(\hat{\boldsymbol{\Theta}}) = 1, \tag{10c}$$

where $\hat{\boldsymbol{\Theta}} = \hat{\boldsymbol{\theta}}\hat{\boldsymbol{\theta}}^{\mathrm{H}}$, $\mathbf{A} = |\frac{1}{\sigma_{\mathrm{B}}^2}|^2\mathbf{H}_{\mathrm{B}}\mathbf{G}\mathbf{w}\mathbf{w}^{\mathrm{H}}\mathbf{G}^{\mathrm{H}}\mathbf{H}_{\mathrm{B}}^{\mathrm{H}}$, $\mathbf{B} = |\frac{1}{\sigma_{\mathrm{E}}^2}|^2\mathbf{H}_{\mathrm{E}}\mathbf{G}\mathbf{w}\mathbf{w}^{\mathrm{H}}\mathbf{G}^{\mathrm{H}}\mathbf{H}_{\mathrm{E}}^{\mathrm{H}}$. (10c) was due to $\hat{\boldsymbol{\Theta}} = \hat{\boldsymbol{\theta}}\hat{\boldsymbol{\theta}}^{\mathrm{H}}$. By ignoring the rank constraint [13], the problem reduces to a linear-fractional programming problem which can be effectively solved with Charnes-Cooper transformation. Therefore, let $u = \frac{1}{1+\mathrm{Tr}(\mathbf{B}\hat{\boldsymbol{\Theta}})}$ and $\hat{\mathbf{U}} = u\hat{\boldsymbol{\Theta}}$, we reformulate convex problem in (11) that can be efficiently solved with cvx [14].

$$\max_{\hat{\mathbf{U}}\succeq 0, u\ge 0} \; u + \mathrm{Tr}(\mathbf{A}\hat{\mathbf{U}}), \tag{11a}$$

$$\text{s.t. } u + \mathrm{Tr}(\mathbf{B}\hat{\mathbf{U}}) = 1, \tag{11b}$$

$$\mathrm{diag}(\hat{\mathbf{U}}) = u. \tag{11c}$$

2) Modified approach: Problem P1b can be simplified to problem P2b because the other terms in the objective function are constants terms.

$$\text{P2b}: \max_{\boldsymbol{\Theta}} \; \gamma_{\mathrm{B}}[n], \tag{12a}$$

$$\text{s.t. } 0 \le \theta_k[n] \le 2\pi. \tag{12b}$$

The solution obtained from solving (12) eventually maximizes the nth information rate of Bob thereby satisfying the objective function in Problem P1b. By expanding $\mathbf{h}_{\mathrm{B}}^{\mathrm{H}}\boldsymbol{\Theta}\mathbf{G}\mathbf{w}$, and following similar derivation as in [9], [15], it is easy to see that the solution to problem P2b is given (13).

$$\boldsymbol{\theta} = \theta_{\mathrm{com}} - \mathbf{u}_{\mathrm{B}} + \mathbf{u}_{\mathrm{G}}, \tag{13}$$

where $\boldsymbol{\theta} = [\theta_1,\ldots,\theta_K]^{\mathrm{T}}$, $\mathbf{u}_{\mathrm{B}} = [\phi_{1\mathrm{B}}^b,\ldots,\phi_{K\mathrm{B}}^b]^{\mathrm{T}}$ and $\mathbf{u}_{\mathrm{G}}$ is the maximum left singular vector corresponding to the rank-1 (low rank) approximation of $\boldsymbol{\Phi}_{\mathrm{G}}$. θ_{com} is an arbitrary phase common to all elements of the IRS. This phase allows for the cancellation of unscrupulous phase elements [9], [16]. Equation (13) shows that the reflection coefficients compensates for the variations of the inter-spacing between the IRS elements, thereby limiting the inter-spacing impact on the reflections.

By the definition of $\boldsymbol{\Theta}$ given in (13) and the knowledge of the channel matrices, we define the nth SNR value at Bob and Eve as:

Proposition 1: $\mathbf{h}_{\mathrm{i}}^{\mathrm{H}}\boldsymbol{\Theta}\mathbf{G} = \boldsymbol{\chi}_{\mathrm{i}}$, where the elements of $\boldsymbol{\chi}_{\mathrm{i}} = [\chi_{1\mathrm{i}},\ldots,\chi_{M\mathrm{i}}]$ are presented in (14a) and (14b) for $\mathrm{i} \in \{\mathrm{B},\mathrm{E}\}$, respectively:

$$\chi_{m\mathrm{B}} = K\sqrt{c_{\mathrm{RB}}c_{m\mathrm{R}}}\exp\left(-j(\phi_{m\mathrm{R}}^a + \phi_{\mathrm{RB}}^a - \theta_{\mathrm{com}})\right), \tag{14a}$$

$$\chi_{m\mathrm{E}} = \sqrt{c_{\mathrm{RE}}c_{m\mathrm{R}}}\exp\left(-j\left(\frac{2\pi}{\lambda}(d_{\mathrm{RE}}+d_{m\mathrm{R}})\right)\right)f(K_{\mathrm{x}},K_{\mathrm{y}}) \times \exp\left(j\left(\theta_{\mathrm{com}} + \frac{A_{\mathrm{x}}(K_{\mathrm{x}}-1)}{2} + \frac{A_{\mathrm{y}}(K_{\mathrm{y}}-1)}{2}\right)\right), \tag{14b}$$

where $u_{\mathrm{G}}^{k_{\mathrm{x}},k_{\mathrm{y}}}$ is the kth element of u_{G}. $f(K_{\mathrm{x}},K_{\mathrm{y}}) = \frac{\sin(\frac{1}{2}K_{\mathrm{x}}A_{\mathrm{x}})\sin(\frac{1}{2}K_{\mathrm{y}}A_{\mathrm{y}})}{\sin(\frac{1}{2}A_{\mathrm{x}})\sin(\frac{1}{2}A_{\mathrm{y}})}$, $A_{\mathrm{x}} = \bar{d}_{\mathrm{x}}(\hat{\mathbf{a}}_{\mathrm{RE}}^{\mathrm{x}} + \hat{\mathbf{a}}_{\mathrm{RB}}^{\mathrm{x}} - \hat{\mathbf{a}}_{m\mathrm{B}}^{\mathrm{x}})$ and $A_{\mathrm{y}} = \bar{d}_{\mathrm{y}}(\hat{\mathbf{a}}_{\mathrm{RE}}^{\mathrm{y}} + \hat{\mathbf{a}}_{\mathrm{RB}}^{\mathrm{y}} - \hat{\mathbf{a}}_{m\mathrm{B}}^{\mathrm{y}})$.

Proof: By substituting and simplifying the expressions for $\mathbf{h}_{\mathrm{i}}$, $\boldsymbol{\Theta}$, and, $\mathbf{G}$ given in equations (5), (13) and (4) respectively, it is easy to see that $\mathbf{u}_{\mathrm{G}}$ in (13) is designed as a rank-1 approximation to cancel out the variations of the columns of matrix $\boldsymbol{\Phi}_{\mathrm{G}}$. However, we know that the rank-1 approximation error of $\mathbf{u}_{\mathrm{G}}$ increases as $r > 0$ since the sensor are randomly placed over large area, hence $|\mathbf{u}_{\mathrm{G}} - \boldsymbol{\Phi}_{\mathrm{G}}(:,m)| \ge 0$. However, from experimentation, for small values of r, $|\mathbf{u}_{\mathrm{G}} - \boldsymbol{\Phi}_{\mathrm{G}}(:,m)| = 0$ allowing the cancellation of $\boldsymbol{\Phi}_{\mathrm{G}}$. This completes the proof of the proposition. ■

Following Proposition 1, we infer that the maximum signal-to-noise ratio (SNR) values at Bob and Eve are

$$\epsilon[n] = \frac{\frac{1}{3\sqrt[3]{2}}\sqrt[3]{2b^3 + 3\sqrt{3}\sqrt{-4b^3d - b^2c^2 + 18bcd + 4c^3 + 27d^2} - 9bc - 27d} - \sqrt[3]{2}(3c - b^2)}{3\sqrt[3]{2b^3 + 3\sqrt{3}\sqrt{-4b^3d - b^2c^2 + 18bcd + 4c^3 + 27d^2} - 9bc - 27d} + \frac{b}{3}}, \tag{15}$$

where $b = \frac{\|\mathbf{\Omega}_{\mathrm{B}}\|}{2\|\mathbf{\Omega}_{\mathrm{A}}\|} + 2\frac{\|\mathbf{q}[n-1]\|}{\|\mathbf{\Omega}_{\mathrm{A}}\|} + \frac{1}{2}$, $c = \frac{\|\mathbf{\Omega}_{\mathrm{B}}\|\|\mathbf{q}[n-1]\| + \|\mathbf{q}[n-1]\|^2}{\|\mathbf{\Omega}_{\mathrm{A}}\|^2} - \frac{\|\mathbf{q}[n-1]\|}{\|\mathbf{\Omega}_{\mathrm{A}}\|}$, $d = \frac{\|\mathbf{\Omega}_{\mathrm{B}}\|}{2\|\mathbf{\Omega}_{\mathrm{A}}\|}\frac{\|\mathbf{q}[n-1]\|^2}{\|\mathbf{\Omega}_{\mathrm{A}}\|^2} + \frac{\|\mathbf{q}[n-1]\|^2}{2\|\mathbf{\Omega}_{\mathrm{A}}\|^2} - \frac{(Z\alpha)^2}{2\|\mathbf{\Omega}_{\mathrm{A}}\|^2}$

$$\gamma_{\mathrm{B}} = \sum_{m=1}^{M} \frac{\bar{P}\varsigma_{\mathrm{B}}\varsigma_k(\rho_0 K)^2}{d_{\mathrm{RB}}^2 d_{\mathrm{mR}}^2}, \tag{16a}$$

$$\gamma_{\mathrm{E}} = \sum_{m=1}^{M} \frac{\bar{P}\varsigma_{\mathrm{E}}\varsigma_k(\rho_0|\zeta|)^2}{d_{\mathrm{RE}}^2 d_{\mathrm{mR}}^2}, \tag{16b}$$

$$|\zeta|^2 = \sum_{k_{\mathrm{x}}=1}^{K_{\mathrm{x}}}\sum_{k_{\mathrm{y}}=1}^{K_{\mathrm{y}}} \exp\Big(j\Big[(k_{\mathrm{x}}-1)\bar{d}_{\mathrm{x}}(\hat{\mathbf{a}}_{\mathrm{RE}}^{\mathrm{x}} + \hat{\mathbf{a}}_{\mathrm{RB}}^{\mathrm{x}} - \hat{\mathbf{a}}_{m\mathrm{R}}^{\mathrm{x}}) + (k_{\mathrm{y}}-1)\bar{d}_{\mathrm{y}}(\hat{\mathbf{a}}_{\mathrm{RE}}^{\mathrm{y}} + \hat{\mathbf{a}}_{\mathrm{RB}}^{\mathrm{y}} - \hat{\mathbf{a}}_{m\mathrm{R}}^{\mathrm{y}}) + u_{\mathrm{G}}^{k_{\mathrm{x}},k_{\mathrm{y}}}\Big]\Big) \overset{(a)}{\leq} K,$$

where $\bar{P} = \frac{P}{\sigma_i^2}$. The bounds in (16) invariably define the bounds of the average secrecy rate (ASR). The equality in (a) represents the worst-case scenario and arises when the channel of Bob and Eve are highly correlated. This may occur if Eve is located at the exact position of Bob.

B. Solving for the beamforming weights, $\mathbf{w}$

The beamforming weights $\mathbf{w}$ are determined for the generic and modified approaches are follow:

1) Generic approach: Taking the eavesdropper's information into consideration, we reformulate problem P1a as

$$\text{P3a}: \quad \max_{\mathbf{w}} \ \left(\frac{1 + \mathbf{w}^{\mathrm{H}}\mathbf{A}\mathbf{w}}{1 + \mathbf{w}^{\mathrm{H}}\mathbf{B}\mathbf{w}}\right), \tag{17a}$$

$$\text{s.t. } \mathbf{w}^{\mathrm{H}}\mathbf{w} \leq P, \tag{17b}$$

where $\mathbf{A} = \frac{1}{\sigma_{\mathrm{B}}^2}(\mathbf{h}_{\mathrm{B}}^{\mathrm{H}}\mathbf{\Theta}\mathbf{G})^{\mathrm{H}}(\mathbf{h}_{\mathrm{B}}^{\mathrm{H}}\mathbf{\Theta}\mathbf{G})$, $\mathbf{B} = \frac{1}{\sigma_{\mathrm{E}}^2}(\mathbf{h}_{\mathrm{E}}^{\mathrm{H}}\mathbf{\Theta}\mathbf{G})^{\mathrm{H}}(\mathbf{h}_{\mathrm{E}}^{\mathrm{H}}\mathbf{\Theta}\mathbf{G})$. This implies that by considering the presence of both Bob and Eve, the optimal $\mathbf{w}^* = \sqrt{P}\mathbf{u}_{\max}$, where $\mathbf{u}_{\max}$ is the eigenvector corresponding to the maximum eigenvalue of the matrix $(\mathbf{B} + \frac{1}{P}\mathbf{I}_M)^{-1}(\mathbf{A} + \frac{1}{P}\mathbf{I}_M)$ [8].

2) Modified approach: Since the IRS can direct signals to specific targets, we consider transmission to Bob only ignoring the presence of Eve. Then the problem P1b reduces to

$$\text{P3b}: \quad \max_{\mathbf{w}} \ (1 + \mathbf{w}^{\mathrm{H}}\mathbf{A}\mathbf{w}), \tag{18a}$$

$$\text{s.t. } \mathbf{w}^{\mathrm{H}}\mathbf{w} \leq P, \tag{18b}$$

where $\mathbf{A} = \frac{1}{\sigma_{\mathrm{B}}^2}(\mathbf{h}_{\mathrm{B}}^{\mathrm{H}}\mathbf{\Theta}\mathbf{G})^{\mathrm{H}}(\mathbf{h}_{\mathrm{B}}^{\mathrm{H}}\mathbf{\Theta}\mathbf{G})$. It is known that the optimal $\mathbf{w}^* = \sqrt{P}\mathbf{u}_{\max}$ is an MRT beamformer towards the UAV, where $\mathbf{u}_{\max}$ is the eigenvector corresponding to the maximum eigenvalue of the channel matrix $\frac{1}{\sigma_{\mathrm{B}}^2}(\mathbf{h}_{\mathrm{B}}^{\mathrm{H}}\mathbf{\Theta}\mathbf{G})^{\mathrm{H}}(\mathbf{h}_{\mathrm{B}}^{\mathrm{H}}\mathbf{\Theta}\mathbf{G})$ [9], [17].

C. Solving for the UAV trajectory, $\mathbf{Q}$

In this subsection, we investigate methods to obtain the trajectory of the UAV carrying the IRS system given that the reflection coefficient, $\mathbf{\Theta}$, and beamforming weights, $\mathbf{w}$ are known.

1) Generic approach: To obtain the trajectory of the UAV, problem P1a is reformulated as problem P4a:

$$\text{P4a}: \quad \max_{\mathbf{Q}} \ \sum_{n=1}^{N}\left[\log_2\left(\frac{1+\gamma_{\mathrm{B}}[n]}{1+\gamma_{\mathrm{E}}[n]}\right)\right] \tag{19a}$$

$$\text{s.t. } \|\mathbf{q}[n] - \mathbf{q}[n-1]\|^2 \leq (Z\alpha)^2. \tag{19b}$$

Note that the problem P4a is non-convex due to the fractional objective. The problem P4a can be solved by introducing an auxiliary variable, β limiting the maximum achievable rate by Eve as shown in (20). The addition of β is required to make the problem tractable. Furthermore, considering that the inter-sensor space is very small compared to the distance to the UAV-IRS system, we can assume for simplification that the UAV trajectory is determined in respect to Alice rather than the individual sensors, $(d_{\mathrm{mR}} \approx d_{\mathrm{AR}})$. Hence, by substituting parameters, (19) was reformulated as (20).

$$\max_{\mathbf{Q},\beta} \ \sum_{n=1}^{N}\left[\log_2\left(\frac{1 + \left(\frac{\bar{P}M(\rho_0\varsigma_{\mathrm{B}}K)^2}{d_{\mathrm{RB}}^2 d_{\mathrm{AR}}^2}\right)[n]}{\beta[n]}\right)\right], \tag{20a}$$

$$\text{s.t. } 1 + \left(\frac{\bar{P}M(\rho_0\varsigma_{\mathrm{E}}K)^2}{d_{\mathrm{RB}}^2 d_{\mathrm{AR}}^2}\right)[n] \leq \beta[n] \tag{20b}$$

$$\|\mathbf{q}[n] - \mathbf{q}[n-1]\|^2 \leq (Z\alpha)^2. \tag{20c}$$

Equation (20) can be solved using Karush-Kuhn-Tucker (KKT) conditions to obtain the optimal trajectory of the UAV as defined in (21).

$$q_{\mathrm{x}}^2[n] + q_{\mathrm{y}}^2[n] = (\epsilon[n]\|\Omega_{\mathrm{A}}\|)^2 - H^2, \tag{21}$$

where ϵ is given in (15) at the top of current page.

Proof: See Appendix A. ■

The closed-form expression for ϵ is given in (15). The solution to (21) can easily be obtained by a linear search algorithm that seeks for pairs of points that satisfy the trajectory constraint in (20c).

2) Modified approach: Problem P1b can be presented in terms of the trajectory as problem P4b:

$$\text{P4b}: \quad \max_{\mathbf{Q}} \ \sum_{n=1}^{N}[\log_2(1+\gamma_{\mathrm{B}}[n])] \tag{22a}$$

$$\text{s.t. } \|\mathbf{q}[n] - \mathbf{q}[n-1]\|^2 \leq (Z\alpha)^2. \tag{22b}$$

The solution to problem P4b can be obtained by solving (21) with the definition for ϵ as:

$$\epsilon = \frac{\|\mathbf{q}_{\mathrm{R}}[n-1]\| \pm Z\alpha}{\|\mathbf{\Omega}_{\mathrm{A}}\|}. \tag{23}$$

Thereafter, a linear search method as described in section III-C1 is employed until the points maximizing the objective function in problem P4b is obtained.

D. Overall Solution

The overall iterative procedure for the generic model is summarised in Algorithm 1 following successive convex optimization (SCA) technique. Similarly, the non-iterative steps to solve the modified model entails sequentially solving for $\mathbf{Q}$ and $\mathbf{\Theta}$ and $\mathbf{w}$ (23), (13) and (18) respectively. The time computational complexity of the iterative Algorithm 1 is computed as $\mathcal{O}(\hat{n}\log\hat{n})$, where $\log\hat{n}$ follows from the iteration and $\hat{n}$ is the number of iterations. However the complexity for the non iterative solution is given as $\mathcal{O}(\hat{n})$.

Algorithm 1 Iterative algorithm for solving $\mathbf{\Theta}$, $\mathbf{w}$, and $\mathbf{Q}$ for the Generic approach

1: Initialize $R_s^0 = 0$, $\mathbf{w}^0$ and $\mathbf{q}^0$ such that the constraints in (7d) and (7c) are respectively satisfied.
2: $\hat{m} \leftarrow 1$, **repeat**
3: Solve (21) with (15) and update $\mathbf{q}$.
4: Compute the locations of the IRS elements.
5: Determine the channel responses from (4) and (5).
6: **for all** n **do**
7: Solve (11) to obtain $\mathbf{\Theta}$.
8: Compute and update $\mathbf{w}$ with III-B1.
9: **end for**
10: Compute R_s as defined in (7a).
11: Compute $e = \left|\frac{R_s^{new} - R_s^{old}}{R_s^{new}}\right|$.
12: $\hat{m} \leftarrow \hat{m} + 1$, **until** $e < 1 \times 10^{-4}$.
13: **Output:** $\mathbf{\Theta}$, $\mathbf{w}$ and $\mathbf{Q}$.

IV. Results and Discussions

In this section, we evaluate the performance of the algorithms via numerical simulations and compared them with baseline schemes. Except when explicitly stated, the parametric settings of the simulation environment are: $H = 100$m, $Z = 3$m/s, $M = 4$, $\mathbf{\Omega}_{\mathrm{A}} = [0, -100, 0]^{\mathrm{T}}$, $\mathbf{\Omega}_{\mathrm{E}} = [-100, 50, 0]^{\mathrm{T}}$ (Uncorrelated), $\mathbf{\Omega}_{\mathrm{E}} = [75, 100, 0]^{\mathrm{T}}$ (Correlated), $\mathbf{\Omega}_{\mathrm{B}} = [80, 100, 0]^{\mathrm{T}}$, $\mathbf{\Omega}_{\mathrm{fixIRS}} = [100, 80, 0]^{\mathrm{T}}$. The legends Scheme 1, Scheme 2, and Fixed refers to the non-iterative approach, Algorithm 1 and a fixed IRS scheme [8] respectively.

Figure 1 presents the trajectory of the UAV as we change the location of Eve. In the sub-figures, we considered 2 cases: when Eve location is far away from Bob and close to Bob. The UAV attempts to find paths that are as far from Eve as possible while maintaining reasonable distance between Alice and Bob to ensure the transmitted signals are received and reflected. When the best safe distance is obtained, the UAV hovers around that location until the end of the simulation. This behaviour of the UAV is similar for different scheduled flight times.

Following the trajectory presented in fig. 1, it was observed in fig. 2 that the longer the UAV flies with the IRS for a given communication, the better the ASR. It has been established in [9] that for aerial IRS, the SNR increases with higher transmit power. However, due to the IRS, we showed that the SNR for Eve declines leading to an increase in the ASR as observed in the rate of the Eve in fig. 4. Figure 2 also provides an insight that scheme 2 performs better than scheme 1 when the channels of Bob and Eve are correlated and uncorrelated.

In fig. 3, the impact of transmit power on the ASR of the system was presented. By comparing the sub-figures, scheme 2 out-performs scheme 1 when the channel quality of Bob and Eve are strong and highly uncorrelated. Similar assertion was presented in fig. 4 while examining the influence of distance between Bob and Eve representing correlation are studied. The correlation referred to the proximity between Bob and Eve. Hence, we further deduced from fig. 4 that for passive eavesdropping, the Scheme 1 perform better when the eavesdropper is strictly correlated to the legitimate receiver. The non-iterative approach failed to secure the communication under the strict correlation.

V. Conclusion

We have demonstrated the effectiveness of deploying a UAV-carried IRS for collecting sensor data from blackout noisy spaces while guaranteeing communications security. We derived the optimal location as well as the reflection coefficients of the IRS elements to improve the secure data transmission performance. The UAV follows a trajectory that can aid in sustaining the secrecy performance while the IRS can further assist secure communication by increasing phase disparity at the eavesdropper. The non-iterative algorithm, for when the eavesdropper is passive, saves huge computation tasks compared to the iterative procedure at a trade-off of lower PLS and restriction on the location of the eavesdropper.

Appendix A

To provide a solution to (20), we express the lower bound for the distances using the reverse triangular inequality and variable change as

$$\begin{aligned}
d_{\mathrm{RE}}^2 d_{\mathrm{AR}}^2 &= \|\mathbf{\Omega}_{\mathrm{E}} - \mathbf{q}_{\mathrm{R}}\|^2 \|\mathbf{q}_{\mathrm{R}} - \mathbf{\Omega}_{\mathrm{A}}\|^2 \\
&\geq (\|\mathbf{\Omega}_{\mathrm{E}}\| - \|\mathbf{q}_{\mathrm{R}}\|)^2 (\|\mathbf{q}_{\mathrm{R}}\| - \|\mathbf{\Omega}_{\mathrm{A}}\|)^2 \\
&= \left(\underbrace{\frac{\|\mathbf{\Omega}_{\mathrm{E}}\|}{\|\mathbf{\Omega}_{\mathrm{A}}\|}}_{\bar{\Omega}_{\mathrm{E}}} - \underbrace{\frac{\|\mathbf{q}_{\mathrm{R}}\|}{\|\mathbf{\Omega}_{\mathrm{A}}\|}}_{\epsilon}\right)^2 \left(\underbrace{\frac{\|\mathbf{q}_{\mathrm{R}}\|}{\|\mathbf{\Omega}_{\mathrm{A}}\|}}_{\epsilon} - 1\right)^2 \|\mathbf{\Omega}_{\mathrm{A}}\|^4 \\
&= (\bar{\Omega}_{\mathrm{E}} - \epsilon)^2 (\epsilon - 1)^2 \|\mathbf{\Omega}_{\mathrm{A}}\|^4, \\
d_{\mathrm{RB}}^2 d_{\mathrm{AR}}^2 &\geq (\bar{\Omega}_{\mathrm{B}} - \epsilon)^2 (\epsilon - 1)^2 \|\mathbf{\Omega}_{\mathrm{A}}\|^4, \\
\|\mathbf{q}_{\mathrm{R}}[n] - \mathbf{q}_{\mathrm{R}}[n-1]\|^2 &\geq (\epsilon - \bar{\Omega}_q)^2 \|\mathbf{\Omega}_{\mathrm{A}}\|^2, \\
\text{where } \bar{\Omega}_q &= \frac{\|\mathbf{q}_{\mathrm{R}}[n-1]\|}{\|\mathbf{\Omega}_{\mathrm{A}}\|}.
\end{aligned}$$

Considering that the trajectory of the UAV is a sequential combination of its location at instantaneous n samples, the objective of (20) can be scaled to obtaining the maximum value at the nth sample. The summation of these isolated optimal points provides the optimal objective value as defined in (20). Hence, by using variable change as defined above, (20) can be rewritten as (A.2) $\forall\ n \in [1, \ldots, N]$.

$$\max_{\epsilon} \ \log_2\left(\frac{1}{\beta} + \frac{\bar{P} M \rho_0^2 \varsigma_{\mathrm{B}}^2 K^2}{\beta(\bar{\Omega}_{\mathrm{B}} - \epsilon)^2 (\epsilon - 1)^2 \|\mathbf{\Omega}_{\mathrm{A}}\|^4}\right), \tag{A.2a}$$

$$\text{s.t.} \ \frac{1-\beta}{|\zeta|^2} + \frac{\bar{P} M \rho_0^2 \varsigma_{\mathrm{E}}^2}{\beta(\bar{\Omega}_{\mathrm{E}} - \epsilon)^2 (\epsilon - 1)^2 \|\mathbf{\Omega}_{\mathrm{A}}\|^4} \leq 0, \tag{A.2b}$$

$$(\epsilon - \bar{\Omega}_q)^2 \|\mathbf{\Omega}_{\mathrm{A}}\|^2 \leq (Z\alpha)^2. \tag{A.2c}$$

Equation (A.2) is differentiable and possibly non-convex due to (A.2a) and (A.2b). However, let ϵ^* and $(\lambda_1^*, \lambda_2^*)$ represent

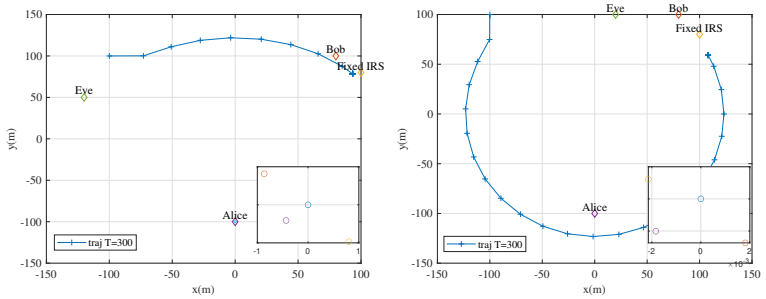

(a) Eve's location is far from Bob (b) Eve's location is close to Bob

Fig. 1: UAV trajectory for different locations of Eve.

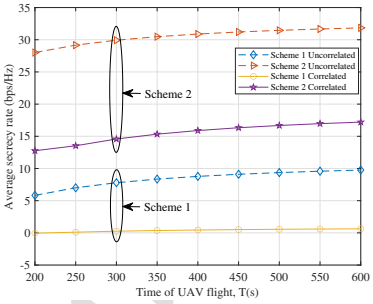

Fig. 2: Impact of flight time for $K = 16$, $r = 1\text{m}$, $\rho_0 = 120\text{dBm}$, and $P = 1\text{dBm}$

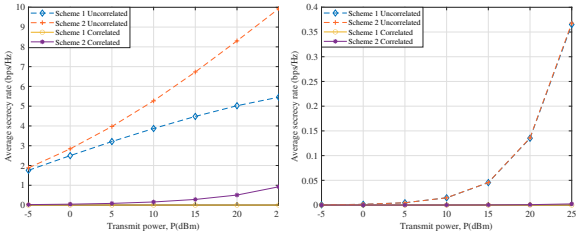

(a) $\rho_0 = 60\text{dBm}$ (b) $\rho_0 = 30\text{dBm}$

Fig. 3: ASR versus transmit power for $K = 16$, $r = 1\text{m}$ and $T = 300\text{s}$.

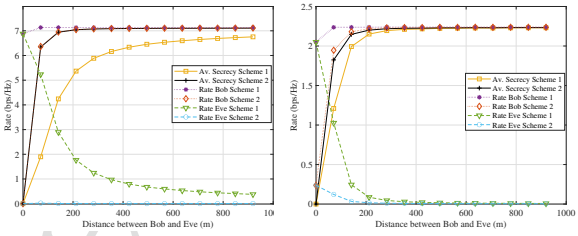

(a) $\rho_0 = 60\text{dBm}$ (b) $\rho_0 = 30\text{dBm}$

Fig. 4: ASR versus correlation between Bob and Eve for $K = 16$, $r = 1\text{m}$, $P = 10\text{dBm}$ and $T = 300\text{s}$.

the primal and dual optimal variables with zero duality gap, the KKT conditions given in (A.3) must be satisfied.

$$\nabla f_0(\epsilon^*) + \lambda_1^* \nabla f_1(\epsilon^*) + \lambda_2^* \nabla f_2(\epsilon^*) = 0, \quad \text{(A.3a)}$$

$$\lambda_1^* f_1(\epsilon^*) = 0, \quad \text{(A.3b)}$$

$$\lambda_2^* f_2(\epsilon^*) = 0. \quad \text{(A.3c)}$$

By using the functions from (22) where f_0 is the objective function and f_1 and f_2 are the constraint functions corresponding to (A.3b) and (A.3c) respectively, we note that $\lambda_1^* = f(\epsilon^*, \lambda_2^*)$ by solving (A.3a), $\lambda_2^* = f(\epsilon^*)$ by solving (A.3b) and substituting λ_1^*. Therefore, by solving (A.3c), we obtain the cubic function $\epsilon^3 - b\epsilon^2 + c\epsilon + d = 0$ with discriminant $\Delta = (bc)^2 + 18(bcd) - 4c^3 - 4b^3 d - 27d^2$; ($\epsilon$, b, c, d has been presented in (15)). Having obtained ϵ, the location of the UAV at the nth sample can be deduced from $\epsilon = \frac{\|\mathbf{q}_\text{R}\|}{\|\mathbf{\Omega}_\text{A}\|}$ which can invariably be modified component-wise to Proposition 1.

Conflict of Interest

The authors declare no conflict of interest in this paper.

References

[1] V. A. Thakor, M. A. Razzaque, and M. R. A. Khandaker, "Lightweight cryptography algorithms for resource-constrained IoT devices: A review, comparison and research opportunities," *IEEE Access*, vol. 9, pp. 28 177–28 193, 2021.

[2] M. R. A. Khandaker and K. Wong, "Robust secrecy beamforming with energy-harvesting eavesdroppers," *IEEE Wireless Communications Letters*, vol. 4, no. 1, pp. 10–13, 2015.

[3] L. Dong, Z. Han, A. P. Petropulu, and H. V. Poor, "Improving wireless physical layer security via cooperating relays," *IEEE Transactions on Signal Processing*, vol. 58, no. 3, pp. 1875–1888, 2010.

[4] C. O. Nnamani, M. R. Khandaker, and M. Sellathurai, "Secrecy rate maximization with gridded UAV swarm jamming for passive eavesdropping," in *2021 IEEE Global Communications Conference (GLOBECOM)*, 2021, pp. 01–06.

[5] J. Chen, Y. Liang, Y. Pei, and H. Guo, "Intelligent reflecting surface: A programmable wireless environment for physical layer security," *IEEE Access*, vol. 7, pp. 82 599–82 612, 2019.

[6] B. Matthiesen, E. Björnson, E. De Carvalho, and P. Popovski, "Intelligent reflecting surface operation under predictable receiver mobility: A continuous time propagation model," *IEEE Wireless Communications Letters*, vol. 10, no. 2, pp. 216–220, 2021.

[7] O. Ozdogan, E. Bjornson, and E. G. Larsson, "Intelligent reflecting surfaces: Physics, propagation, and pathloss modeling," *IEEE Wireless Commun. Lett.*, vol. 9, no. 5, pp. 581–585, 2020.

[8] M. Cui, G. Zhang, and R. Zhang, "Secure wireless communication via intelligent reflecting surface," *IEEE Wireless Commun. Lett.*, vol. 8, no. 5, pp. 1410–1414, 2019.

[9] H. Lu, Y. Zeng, S. Jin, and R. Zhang, "Aerial intelligent reflecting surface: Joint placement and passive beamforming design with 3D beam flattening," *IEEE Trans. Wireless Commun.*, 2020.

[10] H. Long, M. Chen, Z. Yang, B. Wang, Z. Li, X. Yun, and M. Shikh-Bahaei, "Reflections in the sky: Joint trajectory and passive beamforming design for secure UAV networks with reconfigurable intelligent surface," 2020.

[11] A. Li, Q. Wu, and R. Zhang, "UAV-enabled cooperative jamming for improving secrecy of ground wiretap channel," *IEEE Wireless Commun. Lett.*, vol. 8, no. 1, pp. 181–184, Feb. 2019.

[12] C. O. Nnamani, M. R. A. Khandaker, and M. Sellathurai, "UAV-aided jamming for secure ground communication with unknown eavesdropper location," *IEEE Access*, vol. 8, Apr. 2020.

[13] Q. Wu and R. Zhang, "Intelligent reflecting surface enhanced wireless network: Joint active and passive beamforming design," in *2018 IEEE Global Commun. Conf. (GLOBECOM)*, 2018.

[14] M. Grant and S. Boyd, *Recent advances in learning and control*, ser. Lecture Notes in Control and Information Sciences. Springer-Verlag Limited, Mar. 2008, ch. Graph implementations for nonsmooth convex programs, pp. 95–110.

[15] S. Li, B. Duo, X. Yuan, Y.-C. Liang, and M. D. Renzo, "Reconfigurable intelligent surface assisted UAV communication: Joint trajectory design and passive beamforming," *IEEE Wireless Commun. Lett.*, vol. 9, no. 5, pp. 716–720, 2020.

[16] Q. Wu, S. Zhang, B. Zheng, C. You, and R. Zhang, "Intelligent reflecting surface-aided wireless communications: A tutorial," *IEEE Transactions on Communications*, vol. 69, no. 5, pp. 3313–3351, 2021.

[17] K. Zarifi, S. Affes, and A. Ghrayeb, "Collaborative null-steering beamforming for uniformly distributed wireless sensor networks," *IEEE Trans. Signal Process.*, vol. 58, no. 3, pp. 1889–1903, 2010.

Christantus Nnamani: Conceptualization, Methodology, Software, Data curation, Visualization, Investigation, Writing- Original draft preparation, Writing- Reviewing and Editing, Funding acquisition

Muhammad Khandaker: Supervision, Writing- Reviewing and Editing, Project administration

Mathini Sellathurai: Supervision, Resources, Writing- Reviewing and Editing, Funding acquisition

Declaration of interests

☒ The authors declare that they have no known competing financial interests or personal relationships that could have appeared to influence the work reported in this paper.

☐The authors declare the following financial interests/personal relationships which may be considered as potential competing interests: